# Electric quadrupolar contribution to the nuclear spin-lattice relaxation of Au and Ru in Fe

G. Seewald, E. Zech, and H.-J. Körner
*Physik-Department, Technische Universität München, D-85748 Garching, Germany*
(Received 23 February 2004; published 27 August 2004)

The electric quadrupolar contribution to the nuclear spin-lattice relaxation of Au and Ru in Fe was determined by nuclear magnetic resonance on oriented nuclei. The magnetic and quadrupolar parts of the relaxation were separated by the comparison of relaxation measurements on $^{198}$Au and $^{199}$Au and on $^{97}$Ru and $^{103}$Ru in the same sample. The high-field limits of the magnetic relaxation constants were deduced to be $R_m = 1.95\left(^{+30}_{-49}\right)$ (s K)$^{-1}$ for $^{198}$Au and $R_m = 0.48(4)$ (s K)$^{-1}$ for $^{97}$Ru. The high-field limits of the quadrupolar relaxation constants were $R_q = 0.60\left(^{+47}_{-19}\right)$ (s K)$^{-1}$ for $^{199}$Au and $R_q = 0.062(15)$ (s K)$^{-1}$ for $^{103}$Ru. The $R_q$'s deviate distinctly from the predictions of *ab initio* calculations. However, the large systematic underestimation by the calculations that is observed for the magnetic relaxation seems to be absent for the quadrupolar relaxation. The importance of the quadrupolar contribution for the spin-lattice relaxation at impurities in Fe is discussed. In addition, the quadrupole moment of $^{97}$Ru was determined by modulated adiabatic fast passage on oriented nuclei to be $Q(^{97}\mathrm{Ru}) = -0.113(9)$ b.

DOI: 10.1103/PhysRevB.70.064419 PACS number(s): 76.60.Es, 75.50.Bb, 76.80.+y

## I. INTRODUCTION

The nuclear spin-lattice relaxation in metals at low temperatures arises from the scattering of conduction electrons at the nuclear site.[1–4] The scattering can be due to the magnetic-dipolar or electric-quadrupolar parts of the hyperfine interaction. According to the magnitudes of the nuclear magnetic and quadrupole moments, for most isotopes the magnetic relaxation dominates. The magnetic relaxation also dominates, if mainly *s* electrons are scattered. Therefore, the electric quadrupolar part has been neglected in most of the experimental and theoretical work on the spin-lattice relaxation in metals.

Recently several calculations have shown that for a few isotopes with large quadrupole and small magnetic moments a nonnegligible quadrupolar relaxation is expected.[5–7] There is still little experimental information: A quadrupolar relaxation has been reported for $^{97}$Mo in Mo (Ref. 8), $^{121}$Sb and $^{123}$Sb in Sb (Refs. 9 and 10), $^{103}$Ru in Ru (Refs. 11 and 12), and $^{189}$Ir in Fe (Ref. 13).

The motivation for a dedicated study of the quadrupolar relaxation is basically that the combination of both parts of the relaxation offers more information than the magnetic relaxation alone. In particular, there is a close relationship between the quadrupolar relaxation and the part of the magnetic relaxation that arises from the orbital hyperfine interaction.[5,6] The quadrupolar relaxation thus helps to distinguish orbital and nonorbital mechanisms in the magnetic relaxation.

This is, for example, desirable in the case of the spin-lattice relaxation in Fe, where there are two problems—namely, the systematic underestimation of the relaxation rates by the *ab initio* calculations and the magnetic-field dependence. Those problems may result from additional relaxation mechanisms in ferromagnetic metals. In particular direct and indirect spin-wave mechanisms have been discussed.[14–16] But the actual origin of the problems is still not established. The investigation of the quadrupolar relaxation of $^{189}$Ir in Fe showed that its magnitude is in agreement with the *ab initio* calculations, and that its field dependence is distinctly smaller than that of the magnetic relaxation.[13]

To establish those results by more data and to obtain a more complete picture of the role of the quadrupolar relaxation, we measured the magnetic and quadrupolar relaxations of Ru and Au in Fe. Ru and Au were chosen mainly for practical reasons: A convenient way to separate the magnetic and quadrupolar parts of the relaxation is to compare the relaxation rates of two isotopes of the same element. At least one of the isotopes should have a large quadrupole moment and a small magnetic moment. $^{97}$Ru and $^{103}$Ru, and $^{198}$Au and $^{199}$Au are suitable isotope pairs, which can moreover be easily produced in the same sample by neutron irradiation.

In previous studies it was already noted that the experimental relaxation rates of $^{97}$Ru and $^{103}$Ru in Fe and of $^{197}$Au and $^{198}$Au in Fe do not scale with the square of the nuclear *g* factor, as would be expected for a purely magnetic relaxation.[14,17] This was, however, attributed to technical difficulties with certain measurement techniques.

## II. QUADRUPOLAR RELAXATION IN METALS

If there are both a magnetic and a quadrupolar contribution, the nuclear spin-lattice relaxation in metals can be described by three relaxation constants, the magnetic relaxation rate $R_m$ and the quadrupolar relaxation rates $R_q^{(1)}$ and $R_q^{(2)}$ due to $\Delta m = \pm 1$ and $\Delta m = \pm 2$ transitions, respectively. They are defined in such a way that $T_1$, the relaxation time in the high-temperature limit, is given by

$$(T_1 T)^{-1} = R = R_m + R_q^{(1)} + R_q^{(2)}. \tag{1}$$

$R_m$, $R_q^{(1)}$, and $R_q^{(2)}$ depend on the nuclear moments and the spin of the particular isotope. Isotope-independent relaxation constants can be specified by $R_m/g^2$, $R_q^{(1)}/N_q$, and $R_q^{(2)}/N_q$. Here $g$ is the nuclear $g$ factor, defined by $\mu = gI\mu_N$, where $\mu$ is the nuclear magnetic moment, $I$ is the nuclear spin, and $\mu_N$

 ©2004 The American Physical Society

is the nuclear magneton. The dimensionless factor $N_q$ is defined by

$$N_q = \frac{Q^2(2I+3)}{I^2(2I-1)}, \tag{2}$$

where it is assumed that the numerical value of the quadrupole moment $Q$ in units of barns is used.

At the low temperatures of nuclear orientation experiments, the relaxation can no longer be described by a single time constant. Instead, a set of rate equations (the master equation) for the populations $p_m$ of the sublevels must be solved,

$$\frac{\mathrm{d}}{\mathrm{d}t}p_m = \sum_n (W_{n,m}p_n - W_{m,n}p_m), \tag{3}$$

where $W_{m,n}$ is the transition rate from the sublevel with magnetic quantum number $m$ and energy $E_m$ to the sublevel with magnetic quantum number $n$ and energy $E_n$. Due to the low concentration of the probe nuclei of less than $10^{-6}$, the spin-spin relaxation can be neglected in this work.

The transition rates are given by[4,16,18]

$$W_{m,m+1} = \frac{h\nu_{m,m+1}}{2k_B(1-b_{m,m+1})} \times [R_m c^{(m)}_{m,m+1} + R^{(1)}_q c^{(q1)}_{m,m+1}] + R_{\mathrm{rf}} c^{(m)}_{m,m+1},$$

$$W_{m+1,m} = \frac{h\nu_{m,m+1} b_{m,m+1}}{2k_B(1-b_{m,m+1})} \times [R_m c^{(m)}_{m,m+1} + R^{(1)}_q c^{(q1)}_{m,m+1}] + R_{\mathrm{rf}} c^{(m)}_{m,m+1},$$

$$W_{m,m+2} = \frac{h\nu_{m,m+2}}{8k_B(1-b_{m,m+2})}[R^{(2)}_q c^{(q2)}_{m,m+2}],$$

$$W_{m+2,m} = \frac{h\nu_{m,m+2} b_{m,m+2}}{8k_B(1-b_{m,m+2})}[R^{(2)}_q c^{(q2)}_{m,m+2}]. \tag{4}$$

Here $\nu_{i,j}=(E_i-E_j)/h$ is the respective transition frequency and $b_{i,j}=\exp(-h\nu_{i,j}/k_BT)$ is the corresponding Boltzmann factor. The $\nu_{m,m+1}$'s deviate only slightly from the magnetic resonance frequency $\nu_m$, and the $\nu_{m,m+2}$'s only slightly from $2\nu_m$. The coefficients $c^{(m)}_{m,m+1}$, $c^{(q1)}_{m,m+1}$, and $c^{(q2)}_{m,m+2}$ are given by

$$c^{(m)}_{m,m+1} = [I(I+1) - m(m+1)],$$

$$c^{(q1)}_{m,m+1} = \frac{5(2m+1)^2(I+m+1)(I-m)}{(2I+3)(2I-1)}, \tag{5}$$

$$c^{(q2)}_{m,m+2} = \frac{5(I+m+2)[I^2-(m+1)^2](I-m)}{(2I+3)(2I-1)}.$$

$R_{\mathrm{rf}}c^{(m)}_{m,m+1}$ is the additional transition rate that arises from the applied radio frequency (rf) field. If no rf field is applied, $R_{\mathrm{rf}}$ is zero. If only a selected transition is excited by the rf field, $R_{\mathrm{rf}}$ does not vanish only for that transition.

$R^{(1)}_q$, $R^{(2)}_q$, and the contribution of the orbital hyperfine interaction to $R_m$, the orbital relaxation constant $R_o$, are not independent: If intra-atomic shielding effects are neglected, the relative magnitudes of $R^{(1)}_q/N_q$, $R^{(2)}_q/N_q$, and $R_o/g^2$ depend only on the symmetry of the electron wave functions at the Fermi energy $e_F$ and the direction of the quantization axis. Figure 1 shows the relative magnitudes for the case that the relaxation is due to $d$ electrons. The symmetry of the $d$ orbitals is characterized by

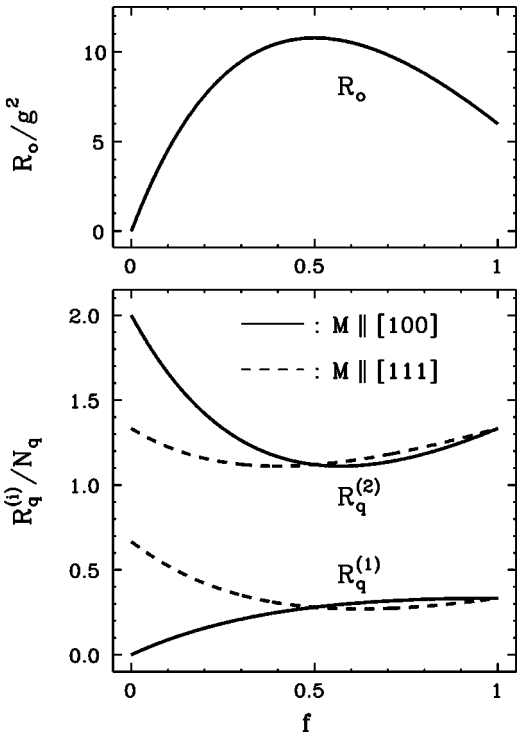


FIG. 1. Orbital and quadrupolar relaxation constants for a given density of states as a function of the amount of $t_{2g}$ symmetry at $e_F$. Only $d$ electrons are considered. The absolute magnitudes of the relaxation constants are arbitrary, but relative to each other the magnitudes are correctly reproduced.

$$f = \frac{N_{t_{2g}}(e_F)}{N_{e_g}(e_F) + N_{t_{2g}}(e_F)}, \tag{6}$$

where $3N_{t_{2g}}(e_F)$ is the partial density of $t_{2g}$ states and $2N_{e_g}(e_F)$ is the partial density of $e_g$ states at $e_F$. $f$ is in general different for the spin-up and spin-down bands. The dependences of $R^{(1)}_q$ and $R^{(2)}_q$ on the direction of the magnetization are illustrated in Fig. 1 by the two extreme cases $M\|[100]$ and $M\|[111]$. $R_q=R^{(1)}_q+R^{(2)}_q$ is independent of the direction of the magnetization.

If the lattice symmetry is cubic and the relaxation is due to $p$ electrons, the following ratios can be derived:[4–6]

$$\frac{R_q/N_q}{R_o/g^2} = 0.546, \tag{7}$$

$$\frac{R^{(1)}_q}{R^{(2)}_q} = 0.25. \tag{8}$$

For $d$ electrons and cubic lattice symmetry, the following relations apply:[4–6]

$$\frac{R_q/N_q}{R_o/g^2} = 0.149\frac{(8-4f+11f^2)}{8f(4-3f)}, \tag{9}$$

$$\frac{R_q^{(1)}}{R_q^{(2)}} = \frac{f(4-f)+8(1-3f+2f^2)F(\boldsymbol{\alpha})}{8-8f+12f^2-8(1-3f+2f^2)F(\boldsymbol{\alpha})}, \tag{10}$$

$$F(\boldsymbol{\alpha}) = (\alpha_x^2\alpha_y^2 + \alpha_y^2\alpha_z^2 + \alpha_z^2\alpha_x^2). \tag{11}$$

Here $\alpha_x$, $\alpha_y$, and $\alpha_z$ are the directional cosines of the magnetization with respect to the cubic axes $x$, $y$, and $z$. $F(\boldsymbol{\alpha})$ varies from 0 for $M\|[100]$ to 1/3 for $M\|[111]$.

## III. MEASUREMENT OF THE QUADRUPOLAR RELAXATION BY NMR-ON

### A. Measurements on different isotopes of the same element

In nuclear magnetic resonance on oriented nuclei (NMR-ON) the resonance is detected via changes in the angular distribution of the $\gamma$ radiation from oriented radioactive probe nuclei.[19] NMR-ON is also a well established technique to measure the nuclear spin-lattice relaxation in ferromagnetic metals.[14,16,20] The frequency modulation (FM) of the rf field is periodically switched on and off to alternately excite the nuclear spins and let them relax back to thermal equilibrium. The relaxation constants are determined via *least squares* fit to the resulting relaxation curve of the $\gamma$ anisotropy. Due to the inhomogeneous broadening of the resonance, practically no nuclei are excited without FM.

The solution of the master equation for the sublevel populations has been described in detail in Refs. 18 and 21. (The procedure that is suggested in Ref. 21 to symmetrize the transition-rate matrix does not work in the presence of both $R_q^{(2)}$ and $R_{\mathrm{rf}}$. However, the diagonalization of the unsymmetrized matrix turned out to be unproblematic.) The angular distribution $W(\theta)$ of the $\gamma$ radiation is given by[22]

$$W(\theta) = 1 + \sum_{k=2,4} A_k B_k P_k(\cos\theta). \tag{12}$$

Here $\theta$ is the angle between the detector and the axis of the nuclear orientation, $P_k$ is the Legendre polynomial of order $k$, the $B_k$'s are linear combinations of the sublevel populations, and the $A_k$'s are the angular distribution coefficients of the particular $\gamma$ transition.

In principle, the only change in the formalism due to the presence of the quadrupolar relaxation are the additional terms in the transition-rate matrix. However, there is now the problem that there are three relaxation constants, $R_m$, $R_q^{(1)}$, and $R_q^{(2)}$, but the information from one relaxation measurement is usually not sufficient to determine more than one relaxation constant.

In this work $R_m$ and $R_q = R_q^{(1)} + R_q^{(2)}$ were separated by relaxation measurements on two isotopes of the same element, whereas $R_q^{(1)}/R_q^{(2)}$ was taken from the theory. The necessary additional information was provided by the ratios of the $R_m$'s and the $R_q$'s of the two isotopes, which were known from the scaling of $R_m$ and $R_q$ with $g^2$ and $N_q$. Thus four relaxation parameters—the $R_m$'s and the $R_q$'s of both isotopes—were fitted to the combined data set consisting of a relaxation measurement on each isotope and the ratios of the $R_m$'s and the $R_q$'s. Of course, this procedure only works, if $N_q/g^2$ is different for the two isotopes, if the nuclear moments are known with sufficient precision, and if $R_q$ is non-negligible at least for one of the isotopes.

The following two systematic errors must be taken into account: First, the value of $R_q$ that is deduced from NMR-ON relaxation curves depends slightly on the assumed ratio $R_q^{(1)}/R_q^{(2)}$, which in turn was known only within certain limits: According to Eq. (10), $R_q^{(1)}/R_q^{(2)}$ was assumed to be in the range 0.11–0.28 for $M\|[100]$, precluding the extreme case $f<0.2$.

Second, due to the hyperfine anomaly (HFA),[23,24] the Fermi-contact interaction does not scale exactly with $g$. Accordingly, the exact scaling of $R_m$ depends on the magnitude of the Fermi-contact contribution to $R_m$, which in turn is *a priori* not known. The static hyperfine field and $\nu_m$ are mainly due to the Fermi-contact interaction.[25] If this is also true for $R_m$, $R_m$ scales with $\nu_m^2$. However, if $R_m$ is dominated by a noncontact contribution, for example, by $R_o$, $R_m$ scales with $g^2$. HFA's are usually smaller than 1% and thus unimportant for relaxation measurements. But this is different for measurements of the quadrupolar relaxation, since a small magnetic moment is the prerequisite for both a large quadrupolar relaxation and a large HFA.

### B. Other signatures of the quadrupolar relaxation

We also investigated by model calculations, whether and in which way differences between the quadrupolar and magnetic relaxations become apparent in the NMR-ON relaxation curves. The main motivation was to find additional signatures by which $R_m$, $R_q^{(1)}$, and $R_q^{(2)}$ can be distinguished. We arrived at the following conclusions.

(i) Within the typical accuracy of NMR-ON measurements, the magnetic and quadrupolar relaxations can usually not be distinguished by the shape of the relaxation curve. There are only a few exceptions. For example, if both $R_q^{(1)}$ and $R_m$ are negligible with respect to $R_q^{(2)}$, the absence of $\Delta m = \pm 1$ transitions prevents the complete relaxation back to equilibrium.

(ii) The apparent magnetic relaxation constant $R_m'$, which is obtained by assuming a purely magnetic relaxation, is in general not simply given by $R_m + R_q^{(1)} + R_q^{(2)}$. Instead $R_m' = R_m + d_q R_q$ applies with $d_q$ typically between 0.55 and 1.00. Thus, relative to the magnetic relaxation, the quadrupolar relaxation tends to be slower in NMR-ON experiments than expected from the respective Korringa constants. $d_q$ depends on $I$, $T$, $R_{\mathrm{rf}}$, $A_4/A_2$, $R_q/R_m$, and $R_q^{(1)}/R_q^{(2)}$. The dependences on $T$ and $R_{\mathrm{rf}}$ are, however, too small for a reliable separation of $R_m$, $R_q^{(1)}$, and $R_q^{(2)}$ by relaxation measurements at different temperatures or rf-excitation strengths.

(iii) It is well known from perturbed angular correlation studies that $R_m$, $R_q^{(1)}$, and $R_q^{(2)}$ contribute with different weights to the relaxations of the $k=2$ and $k=4$ terms of Eq. (12).[26] This effect can be used to distinguish the contributions. However, it is of little use for NMR-ON studies, because for isotopes with appreciable quadrupolar contribution

to the relaxation, the $k=4$ term is usually too small for a reasonably accurate determination of its relaxation behavior. This is due to the small magnetic moments of these isotopes, which lead to small degrees of nuclear orientation, which in turn strongly suppress especially the $k=4$ term.

(iv) $R_m$, $R_q^{(1)}$, and $R_q^{(2)}$ are also weighted differently according to which transitions are excited by the rf field. Therefore, the relaxation constants can be separated by a combination of relaxation measurements that employ different selective excitations and/or nonselective excitation. This method has been used in relaxation measurements by nuclear quadrupole resonance.[9,10] There are, however, some practical limitations to its application to NMR-ON:

First, the transition frequencies must be different. This is in principle the case, since a small spin-orbit-induced electric field gradient (spin-orbit EFG) gives rise to a quadrupole splitting of the resonance into $2I$ equidistant subresonances. The resonance frequencies are given by

$$\nu_{m,m+1} = \nu_m - \Delta\nu_Q(m + 1/2), \tag{13}$$

where $\Delta\nu_Q$ is the subresonance separation. $\nu_{I-1,I}$ is referred to as the $\nu_1$ resonance, $\nu_{I-2,I-1}$ as the $\nu_2$ resonance, and so on. But often the subresonances are not sufficiently well separated because the inhomogeneous broadening of the resonance is larger than $\Delta\nu_Q$.

Second, the resonance amplitudes must be large enough for reasonably accurate relaxation measurements. This is a serious limitation, since the resonance strength in NMR-ON spectra is often largely concentrated in the $\nu_1$ resonance. But also the resonance amplitude for nonselective excitation may become too small, if a relatively large FM is required to excite all subresonances and the rf power per frequency unit is correspondingly reduced. That was in this work the case for $^{199}$Au.

Third, the achievable accuracy is rather modest. For example, in Ref. 13 the relaxation behaviors of $^{189}$IrFe after nonselective excitation and after the excitation of the $\nu_1$ resonance were compared and $R_q^{(1)}/R_q^{(2)}=0.17(9)$ was deduced. This is less stringent than Eq. (10) in combination with the assumption $f>0.2$.

## IV. EXPERIMENTAL DETAILS

The samples were 1 $\mu$m thick cold rolled polycrystalline foils of the respective dilute Fe alloy. The RuFe sample contained 0.2 at.% Ru (0.1 at. % $^{96}$Ru and 0.1 at. % $^{102}$Ru), the AuFe sample contained 0.01 at. % Au and 0.1 at. % Pt. Due to a special sample preparation,[27] the crystallographic orientation was nearly uniform. The foil surface was a (100) plane. The [110] directions within the surface were parallel and perpendicular to the rolling direction. The angular spreads (full width of half maximum) of the crystallographic orientations around this nominal orientation were only about 8°.

The radioactive probe nuclei were produced by neutron irradiation. After the irradiation the samples were annealed for 1 h at 700 °C, mounted into a $^3$He-$^4$He dilution refrigerator, and cooled down to temperatures below 10 mK. The temperature was measured by a $^{60}$CoCo (hcp) nuclear orientation thermometer. The $\gamma$ anisotropy was measured by four Ge detectors, placed at 0°, 90°, 180°, and 270° with respect to the direction of the magnetic field. The count-rate ratio

$$\epsilon = \frac{W(0\,^\circ) + W(180\,^\circ)}{W(90\,^\circ) + W(270\,^\circ)} - 1$$

was used to analyze the data. The magnetic field was applied in the foil plane along the [100] or [110] directions ([100] or [110] geometry).

The frequency was doubly modulated: In addition to the 100 Hz FM with the desired bandwidth, a second 1 Hz FM with bandwidth ±200 Hz was applied. The second FM served to destroy, together with the statistical FM noise of the rf synthesizer, any phase coherence between the rf field and the spin system. The variation of $R_{\rm rf}$ across the sample due to the skin effect was taken into account by analyzing the relaxation data for different assumptions on the skin depth. It turned out that the choice of the skin depth had only a negligible influence on the deduced relaxation constants and the quality of the fit.

The magnetic field dependence of the spin-lattice relaxation was described assuming that the relaxation rate is the sum of a high-field limit and a contribution that is proportional to $\eta^\xi$, where $\eta$ is the nuclear magnetic resonance (NMR) enhancement factor. In the [100] geometry $\eta$ is proportional to $(B_a+B_{\rm ext})^{-1}$ and one obtains

$$R_i = R_i(\infty) + [R_i(0) - R_i(\infty)]\left(\frac{B_a}{B_{\rm ext} + B_a}\right)^\xi. \tag{14}$$

Here $R_i$ represents $R_m$ or $R_q$, $B_a=0.059$ T is the anisotropy field in Fe, $R_i(\infty)$ is the high-field limit, and $R_i(0)$ is the relaxation constant at zero field. This description is a generalization of the so-called enhancement factor model (EFM), where $\xi=2$ is assumed and which has successfully been applied in the past.[14,28]

$R_i(\infty)$ must be compared with the results of *ab initio* calculations, since the relaxation is field independent within the theoretical framework of those calculations. Although the origin of the $\eta$ dependent contribution is not specified within the EFM, displacements of the magnetization probably play a central role, since $\eta$ is a measure of the susceptibility to such displacements.

## V. MEASUREMENTS

### A. NMR-ON and MAPON measurements on $^{97}$Ru and $^{103}$Ru

The resonances of $^{97}$Ru and $^{103}$Ru were measured in the [100] and [110] geometries. Figure 2 shows NMR-ON spectra in the [100] geometry. To determine the unknown quadrupole moment of $^{97}$Ru, the quadrupole splittings of $^{97}$Ru and $^{103}$Ru were determined by modulated adiabatic fast passage on oriented nuclei (MAPON).[29–31] MAPON spectra in the

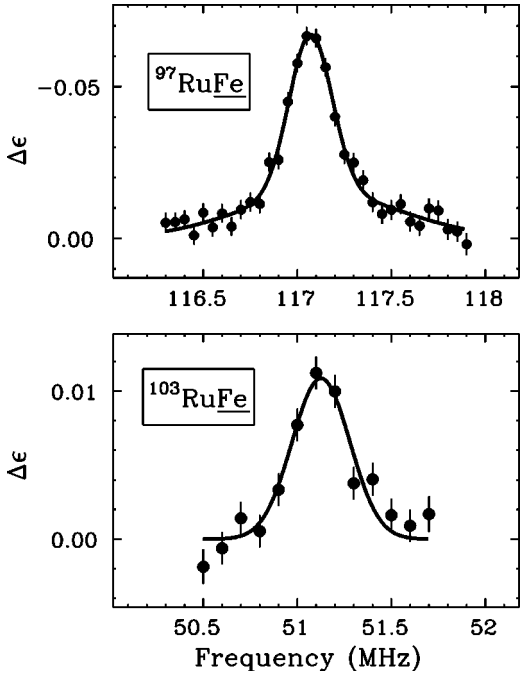


FIG. 2. $^{97}$Ru and $^{103}$Ru in Fe: NMR-ON spectra in the [100] geometry at $B_{ext}=0.2$ T. The larger relative linewidth of the $^{103}$Ru resonance is due to the inhomogeneous broadening of the quadrupole splitting. To obtain the resonance effect $\Delta\epsilon$, the $\gamma$ anisotropy was measured with and without FM and the respective $\epsilon$'s were subtracted from each other.

[110] geometry are shown in Fig. 3. The MAPON spectra can, apart from a prefactor and an offset, be identified with the integral

$$\int_0^{\Delta\nu} [P(\Delta\nu_Q) + P(-\Delta\nu_Q)]\, d\Delta\nu_Q,$$

where $P(\Delta\nu_Q)$ is the distribution of the subresonance separation.[29,32] The signs of the quadrupole splittings were determined from the shapes of the relaxation curves after adiabatic fast passages (AFP's) of opposite sweep directions.[32,33] Figure 4 shows the respective relaxation curves in the [100] geometry.

Using the fact that the MAPON spectra of $^{97}$Ru and $^{103}$Ru are transformable into each other by the multiplication of the $\Delta\nu$ scale by the ratio of the quadrupole splittings, the following value of that ratio was deduced from the comparison of the MAPON spectra of both isotopes,

$$\Delta\nu_Q(^{97}\mathrm{Ru})/\Delta\nu_Q(^{103}\mathrm{Ru}) = -0.0545(37).$$

Using $Q(^{103}\mathrm{Ru}) = +0.62(3)$ b (Ref. 34), the quadrupole moment of $^{97}$Ru is given by

$$Q(^{97}\mathrm{Ru})/Q(^{103}\mathrm{Ru}) = -0.182(12),$$

$$Q(^{97}\mathrm{Ru}) = -0.113(9)\ \mathrm{b}.$$

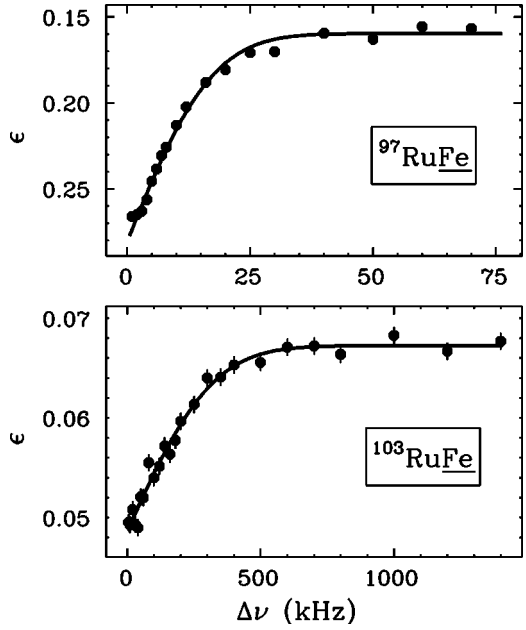


FIG. 3. $^{97}$Ru and $^{103}$Ru in Fe: MAPON spectra in the [110] geometry at $B_{ext}=0.1$ T. Measurements were performed for both sweep directions and the data from an equal number of sweep-up and sweep-down runs were added.

Since, in contrast to previous measurements on RuFe, the electric hyperfine interaction was investigated and measurements were performed for different directions of the magnetization, the hyperfine splitting frequencies may also be of interest. They are listed in Table I.

The determination of $\Delta\nu_Q^{(0)}$, defined as the center of $P(\Delta\nu_Q)$, suffered from the fact that $P(\Delta\nu_Q)$ was inhomogeneously broadened by more than 100%. In this case, which is often encountered in Fe and Ni, the MAPON spectrum can

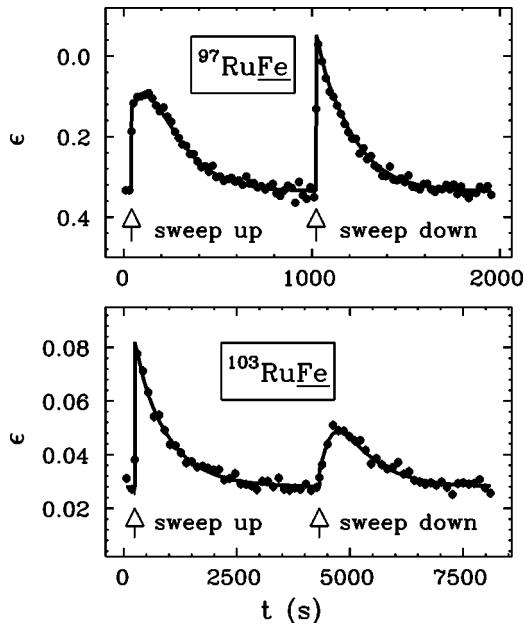


FIG. 4. $^{97}$Ru and $^{103}$Ru in Fe: AFP relaxation curves in the [100] geometry at $B_{ext}=0.1$ T.

TABLE I. Magnetic and electric hyperfine splitting frequencies of $^{97}$Ru and $^{103}$Ru in Fe at $B_{ext}=0.2$ T.

| Isotope | Geometry | $\nu_m$ (MHz) | $\Delta\nu_Q^{(0)}$ (MHz) |
|---|---|---|---|
| $^{97}$Ru | [100] | 117.081(8) | +0.003…+0.012 |
| | [110] | 117.120(8) | +0.001…+0.011 |
| $^{103}$Ru | [100] | 51.01(8) | −0.22…−0.05 |
| | [110] | 50.95(9) | −0.21…−0.02 |

be described by a broad range of $\Delta\nu_Q^{(0)}$'s, including $\Delta\nu_Q^{(0)}=0$, almost equally well. Only an upper limit of $|\Delta\nu_Q^{(0)}|$ can be deduced from the MAPON spectrum and, in combination with the AFP data, also a lower limit and the sign.[32] In the [100] geometry those limits correspond to a spin-orbit EFG between $-0.31\times10^{16}$ and $-0.06\times10^{16}$ V/cm$^2$.

The quoted $\nu_m$'s are already corrected for the displacement of the resonance by the unresolved quadrupole splitting. The results for $^{97}$Ru point to a small anisotropy of the hyperfine field of RuFe:

$$B_{HF}(M\parallel[100]) - B_{HF}(M\parallel[110]) = +0.016(5)\ \text{T}.$$

### B. Relaxation measurements on $^{97}$Ru and $^{103}$Ru

All relaxation measurements were performed in the [100] geometry. The relaxation curves at $B_{ext}=0.2$ T are shown in Fig. 5. At this field the frequency was modulated between 116.8 MHz and 117.4 MHz and between 50.33 MHz and 51.53 MHz for $^{97}$Ru and $^{103}$Ru, respectively. $R_m$ and $R_q$ were separated using the ratios

$$R_m(^{97}\text{Ru})/R_m(^{103}\text{Ru}) = 5.276(19),$$

$$R_q(^{97}\text{Ru})/R_q(^{103}\text{Ru}) = 0.0079(10),$$

which were deduced from the ratios of the magnetic resonance frequencies and quadrupole moments. Figure 6 shows the relaxation constants as a function of the magnetic field.

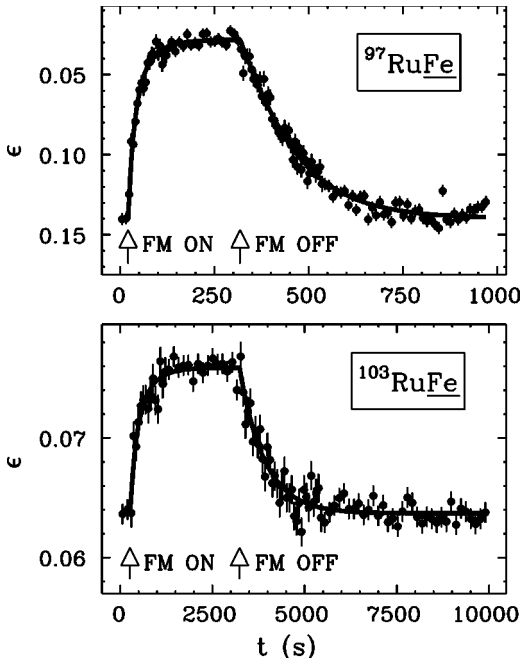


FIG. 5. $^{97}$Ru and $^{103}$Ru in Fe: NMR-ON relaxation curves in the [100] geometry at $B_{ext}=0.2$ T. $T=10.0(2)$ mK for $^{97}$Ru and $T=7.4(2)$ mK for $^{103}$Ru.

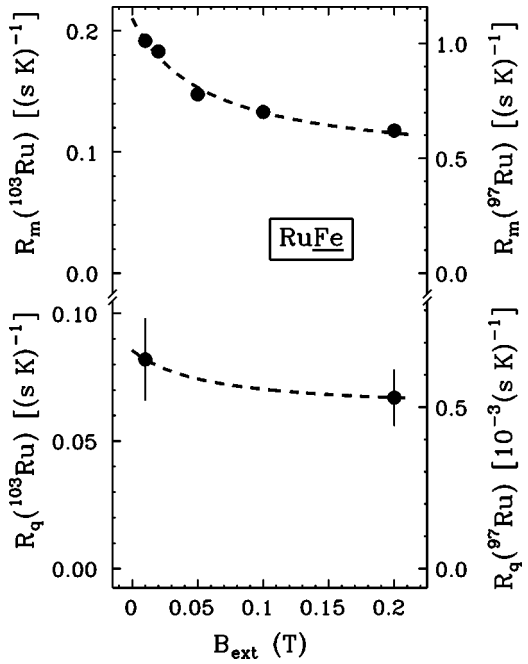


FIG. 6. Magnetic and quadrupolar relaxation constants of $^{97}$Ru and $^{103}$Ru in Fe in the [100] geometry. The dashed curves describe the data by Eq. (14).

The contribution of $R_q$ to the relaxation of $^{97}$Ru turned out to be negligible. The relaxation of $^{97}$Ru thus directly gave the magnetic relaxation constant. But even for $^{103}$Ru, $R_q$ was distinctly smaller than $R_m$, which considerably reduced the statistical accuracy of the determination of $R_q$.

Relaxation measurements on $^{97}$Ru were performed for $B_{ext}=0.01$ T, 0.02 T, 0.05 T, 0.1 T, 0.2 T, 0.4 T, and 0.8 T. Using Eq. (14), the *least squares* fit to the data yielded $\xi=1.05(25)$, $R_m(\infty)=0.48(4)$ (s K)$^{-1}$, and $R_m(0)=1.11(5)$ (s K)$^{-1}$. $R_m(\infty)$ is in agreement with the literature value $R_m(\infty)=0.494(14)$ (s K)$^{-1}$ for $^{97}$Ru.[14]

Due to the much smaller $\gamma$ anisotropy of $^{103}$Ru, only two relaxation measurements could be performed on this isotope. Therefore, the quadrupolar relaxation could be determined only for $B_{ext}=0.01$ T and 0.2 T. The systematic error of $R_q$ due to the uncertainty in $R_q^{(1)}/R_q^{(2)}$ and the neglect of the HFA was of the order of 5% and thus much smaller than the statistical error. Assuming that the field dependence of $R_q$ has the same form, but not necessarily the same amplitude as the field dependence of $R_m$, $R_q(\infty)(^{103}\text{Ru})=0.062(15)$ (s K)$^{-1}$ and $R_q(0)/R_q(\infty)=1.4(5)$ were deduced. No conclusions can

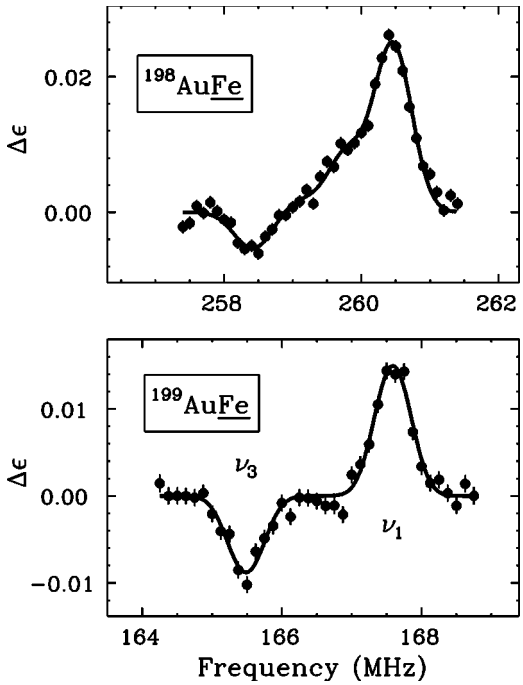


FIG. 7. $^{198}$Au and $^{199}$Au in Fe: NMR-ON spectra in the [100] geometry at $B_{ext}=0.1$ T.

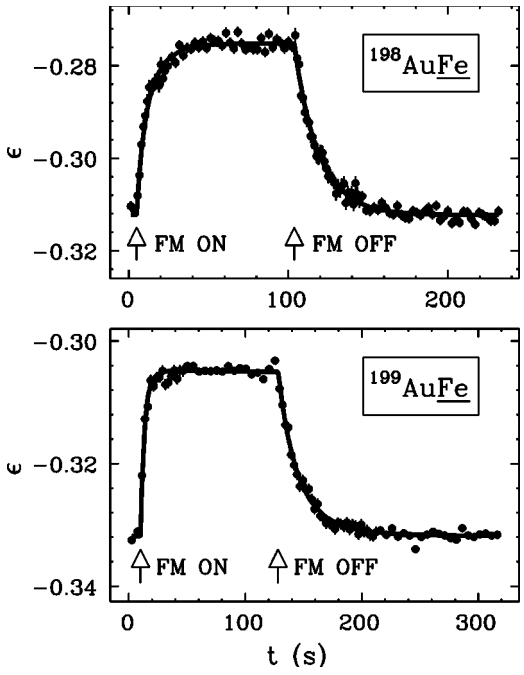


FIG. 8. NMR-ON relaxation curves of $^{198}$Au (411 keV transition) and $^{199}$Au (158 keV transition) in the [100] geometry at $B_{ext}=0.2$ T. For $^{199}$Au only the $\nu_1$ resonance was excited. $T=19.7(4)$ mK for $^{198}$Au and $T=18.7(4)$ mK for $^{199}$Au.

be drawn on the field dependence of the quadrupolar relaxation, since $R_q(0)/R_q(\infty)$ is not significantly different from both 1 and $R_m(0)/R_m(\infty)=2.31(22)$.

### C. Relaxation measurements on $^{198}$Au and $^{199}$Au

NMR-ON spectra of $^{198}$Au and $^{199}$Au are shown in Fig. 7. The subresonances were sufficiently well separated for the selective excitation of individual subresonances only for $^{199}$Au. Accordingly, in the relaxation measurements on $^{198}$Au all subresonances were excited. In the relaxation measurements on $^{199}$Au only the $\nu_1$ resonance was excited, since it provided by far the largest resonance effects. At $B_{ext}=0.1$ T, for example, the frequency was modulated between 257.14 MHz and 261.74 MHz for $^{198}$Au and between 167.27 MHz and 167.97 MHz for $^{199}$Au.

Relaxation measurements were performed in the [100] geometry at $B_{ext}=0.01$ T, 0.1 T, and 0.2 T. The relaxation curves at $B_{ext}=0.2$ T are shown in Fig. 8. To separate $R_m$ and $R_q$, the following ratios were used:

$$R_q(^{198}\mathrm{Au})/R_q(^{199}\mathrm{Au}) = 0.688(6),$$

$$R_m(^{198}\mathrm{Au})/R_m(^{199}\mathrm{Au}) = 2.687(7),$$

if $R_m \propto g^2$ was assumed, and

$$R_m(^{198}\mathrm{Au})/R_m(^{199}\mathrm{Au}) = 2.427(1),$$

if $R_m \propto \nu_m^2$ was assumed. The ratio of the quadrupole moments was taken from Ref. 31, the ratio of the $g$ factors from Ref. 35, and the ratio of the $\nu_m$'s from the NMR-ON measurements. Figure 9 shows the relaxation constants as a function of the magnetic field.

The quadrupolar contribution to the relaxation was nonnegligible for both $^{198}$Au and $^{199}$Au. But even for $^{199}$Au it was smaller than the magnetic contribution. The field dependence of the relaxation was described by Eq. (14). It was assumed that it has the same form, but not necessarily

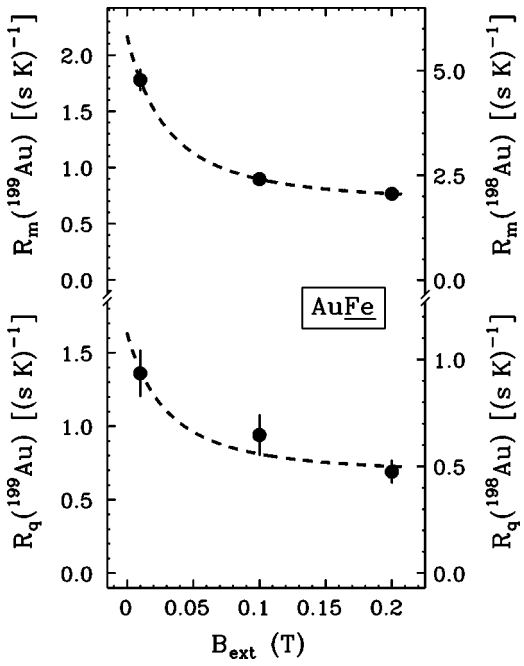


FIG. 9. Magnetic and quadrupolar relaxation constants of $^{198}$Au and $^{199}$Au in Fe in the [100] geometry. $R_q^{(1)}/R_q^{(2)}=0.25$ and $R_m \propto g^2$ were assumed. The dashed curves describe the field dependence according to Eq. (14).

TABLE II. AuFe: High-field limits and field dependences of the magnetic and quadrupolar relaxations for different scalings of $R_m$ and values of $R_q^{(1)}/R_q^{(2)}$.

| Scaling of $R_m$ | $R_q^{(1)}/R_q^{(2)}$ | $R_m(\infty)(^{198}\mathrm{Au})$ $[(\mathrm{s\,K})^{-1}]$ | $R_q(\infty)(^{199}\mathrm{Au})$ $[(\mathrm{s\,K})^{-1}]$ | $R_m(0)/R_m(\infty)$ | $R_q(0)/R_q(\infty)$ |
|---|---|---|---|---|---|
| $\propto g^2$ | 0.28 | 1.88(27) | 0.64(11) | 3.1(5) | 2.5(5) |
| | 0.25 | 1.84(29) | 0.67(12) | 3.2(6) | 2.5(5) |
| | 0.11 | 1.78(32) | 0.90(17) | 3.3(7) | 2.1(5) |
| $\propto \nu_m^2$ | 0.28 | 1.98(27) | 0.51(10) | 3.1(5) | 2.3(6) |
| | 0.25 | 1.95(28) | 0.53(10) | 3.1(5) | 2.3(6) |
| | 0.11 | 1.87(34) | 0.68(13) | 3.3(7) | 2.0(6) |

the same amplitude for $R_m$ and $R_q$. The exponent of the $\eta^{\xi}$ term was $\xi = 2.0(\overline{8})$, where the large error is a consequence of the fact that it is difficult to determine the form of the field dependence from relaxation data for only three different fields.

The deduced $R_q$'s depended significantly on $R_q^{(1)}/R_q^{(2)}$ and the scaling of $R_m$. Those quantities are *a priori* known only within certain limits, but they are predicted by every complete theory. Therefore, we quote in Table II the high-field limits and field dependences for several different assumptions. $R_q^{(1)}/R_q^{(2)} = 0.25$ and a scaling of $R_m$ between $\propto \nu_m^2$ and $\propto g^2$ were regarded as the most probable situation. Permitting also other assumptions, $R_q(\infty)(^{199}\mathrm{Au}) = 0.60(^{+47}_{-19})$ $(\mathrm{s\,K})^{-1}$ was adopted as the final result for the high-field limit of the quadrupolar relaxation.

The results for $R_m(\infty)(^{198}\mathrm{Au})$ (third column of Table II) agree with the more precise literature value $R_m(\infty)(^{198}\mathrm{Au}) = 1.96(8)$ $(\mathrm{s\,K})^{-1}$.[14] However, if the quadrupolar relaxation would have been neglected, $R_m(\infty)(^{198}\mathrm{Au}) = 2.15(28)$ $(\mathrm{s\,K})^{-1}$ would have been obtained. This shows that the neglect of the quadrupolar relaxation leads to an overestimation of $R_m$ by 12(5)% and that the literature value should be corrected accordingly.

The field dependence $R_q(0)/R_q(\infty)$ (last column of Table II) is significantly different from 1. However, the data are not accurate enough to decide whether the field dependences of $R_q$ and $R_m$ are similarly strong or whether the field dependence of $R_q$ is considerably smaller as in the case of IrFe.[13]

## VI. DISCUSSION

The quadrupolar relaxation is now known for RuFe. IrFe, and AuFe. The second and third columns of Table III list the moment-independent high-field limits of the magnetic and quadrupolar relaxations of those systems.

### A. Information on other relaxation mechanisms

*Ab initio* calculations underestimate the relaxation rates in Fe by a factor of 3–5 for the 5*d* impurities and by about a factor of 2 for the 4*d* impurities.[14] One aim of this work was to find out if the same problem also occurs for the quadrupolar part of the relaxation. This information would delimit the range of relaxation mechanisms that can be made responsible: According to the *ab initio* calculations, the relaxation via the orbital hyperfine interaction dominates the spin-lattice relaxation of the transition-metal impurities.[36] If the problem arises from an incorrect description of that mechanism, it should also occur with the quadrupolar relaxation because of the close relationship between both relaxation mechanisms. In contrast, if the problem is due to a so far undiscovered or grossly underestimated nonorbital relaxation mechanism, it should be absent for the quadrupolar relaxation.

To compare the quadrupolar relaxation with the *ab initio* calculations, the theoretical quadrupolar relaxation rate $R_q^{\mathrm{the}}$ had to be inferred indirectly from the theoretical orbital relaxation rate $R_o^{\mathrm{the}}$. Dedicated calculations of the quadrupolar

TABLE III. Experimental and theoretical high-field limits of the magnetic and quadrupolar relaxation of RuFe, IrFe, and AuFe. $R_o^{\mathrm{the}}$ was taken from the *ab initio* calculations of Ref. 36. Within those calculations the orbital and the total magnetic relaxation are almost identical. $R_q^{\mathrm{the}}$ was derived from $R_o^{\mathrm{the}}$ as described in the text.

| System | $R_m(\infty)/g^2$ $(\mathrm{s\,K})^{-1}$ | $R_q(\infty)/N_q$ $(\mathrm{s\,K})^{-1}$ | $R_o^{\mathrm{the}}/g^2$ $(\mathrm{s\,K})^{-1}$ | $R_q^{\mathrm{the}}/N_q$ $(\mathrm{s\,K})^{-1}$ | $(R_q(\infty)/N_q)/(R_m(\infty)/g^2)$ |
|---|---|---|---|---|---|
| RuFe | 4.98(14)[a] | 0.121(29) | 2.4 | 0.31–0.67 | 0.024(6) |
| IrFe | 13.8(7)[b] | $0.45(^{+21}_{-12})$[b] | 3.3 | 0.43–0.92 | $0.033(^{+15}_{-9})$ |
| AuFe | $22(^{-5}_{+4})$ | $1.7(^{+14}_{-5})$ | 3.1 | 0.40–0.86 | $0.08(^{+8}_{-3})$ |

[a]Reference 14.
[b]Reference 13.

relaxation of the 5*d* impurities in Fe have been reported in Ref. 7, but there is probably a problem with those calculations, since the calculated $R_q/R_o$'s were much smaller than it should be possible according to Eqs. (7) and (9). Therefore, the $R_o^{\text{the}}$'s from Ref. 36 (fourth column of Table III) were converted into the respective $R_q^{\text{the}}$'s via Eq. (9). The fifth column of Table III lists the ranges for $R_q^{\text{the}}/N_q$ that were derived assuming $f>0.15$.

For IrFe it had been found that $R_q$ is well reproduced by the *ab initio* calculations.[13] The new data on RuFe and AuFe provide a more refined picture. They confirm that $R_q$ is not systematically underestimated by the calculations. But they also show that $R_q$ is in general not well reproduced: $R_q$(RuFe) is distinctly smaller and $R_q$(AuFe) is distinctly larger than predicted by the calculations. This suggests that the description of $R_q$ and $R_o$ is basically correct. But the accuracy of the calculations seems to be insufficient to reproduce those relaxation constants for each particular system.

### B. Importance of the quadrupolar contribution to the relaxation

The ratio $R_q/R_o$ can also be used to estimate the quadrupolar part of the spin-lattice relaxation, if experimental information is not available.[6] It can be calculated via the Eqs. (7) and (9). In Eq. (9) $f=0.5$ can be assumed for simplicity. At the beginning of each transition-metal series $R_o$ and $R_q$ are probably due to the *p* electrons and Eq. (7) should be used.[6,36] A compilation of the $(R_q/R_o)$'s of the transition-metal isotopes reveals that a non-negligible quadrupolar contribution to the relaxation can be expected only for a few isotopes, in particular 5*d* isotopes, with large quadrupole and small magnetic moments.

In addition, $R_o$ is not necessarily the only important contribution to $R_m$, and $R_q/R_m$ is in general smaller than $R_q/R_o$. The respective reduction factors $R_o/R_m$ can be deduced from the experimental values of $(R_q/N_q)/(R_m/g^2)$, which are listed in the last column of Table III, by dividing them by

$$(R_q/N_q)/(R_o/g^2) = 0.130,$$

which is predicted by Eq. (9) for $f=0.5$. The precise value of $R_o/R_m$ obviously depends on the impurity,but a similar order of magnitude is also expected for the other impurities in Fe. That order of magnitude and a compilation of the $(R_q/R_o)$'s was used to derive the order of magnitude of $R_q/R_m$ for the transition-metal isotopes that are suitable for spin-echo NMR (SE-NMR) or NMR-ON measurements. This revealed (i) the possibilities for further studies of the quadrupolar relaxation and (ii) the need to reinterprete known relaxation constants.

If we require $R_q/R_m>0.3$ for a reliable determination of $R_q$, suitable isotope pairs exist for Pt, Os, W, Ta, and Lu, apart from Au and Ir. For the Hg and Re isotopes, $R_q$ is not large enough. Hf is not soluble in Fe, which prevents the use of the stable Hf isotopes. Nevertheless, $R_q$ can be determined for almost the complete 5*d* series. In contrast, Ru seems to be the only 3*d* or 4*d* impurity where $R_q$ is accessible by the experiment.

The relaxation constants of the transition-metal impurities in Fe are compiled in Ref. 14. Since they have been interpreted as purely magnetic relaxation constants, the deduced values of $R_m/g^2$ are probably in several cases significantly too large. The deviation is known for Ir and Au: The literature values of $R_m/g^2$ for IrFe and AuFe, which were derived from relaxation data on $^{192}$Ir and $^{198}$Au, are too large by 5(2)% and 12(5)%, respectively. For the other systems only estimates are possible: The literature values of $R_m/g^2$ are probably too large by a factor of 2–4 for WFe, where $R_m$ was derived from data on $^{187}$W, by 20–80 % for TaFe and PtFe, where $R_m$ was derived from data on $^{182}$Ta, $^{183}$Ta, and $^{191}$Pt, and be several % for PdFe, ReFe, and OsFe, where $R_m$ was derived from data on $^{105}$Pd, $^{186}$Re, and $^{193}$Os.

Discrepancies between the relaxation constants from SE-NMR measurements and those from NMR-ON and thermal cycling measurements led to the conclusion that the SE-NMR technique yields systematically too large relaxation constants for the 5*d* impurities.[14] However, if the quadrupolar relaxation is taken into account, this conclusion turns out to be incorrect and the discrepancies are at least in part removed. Quantitative conclusions are possible for IrFe and AuFe. Taking only the literature value of $R_m/g^2$ from Ref. 14, $R(^{193}\text{Ir})=0.19(1)\ (\text{s K})^{-1}$ would be predicted. This is much smaller than the SE-NMR result, $R(^{193}\text{Ir})=0.62(6)\ (\text{s K})^{-1}$ (Ref. 37). However, taking $R_m/g^2$ and $R_q/N_q$ from Table III, $R(^{193}\text{Ir})=0.58(13)\ (\text{s K})^{-1}$ is predicted, in agreement with the SE-NMR result. Similarly, $R(^{197}\text{Au})=0.22(1)\ (\text{s K})^{-1}$ would be expected from the literature value of $R_m/g^2$ of AuFe alone, whereas $R(^{197}\text{Au})=0.89(^{+52}_{-20})\ (\text{s K})^{-1}$ is predicted with the relaxation constants of Table III. The SE-NMR result, $R(^{197}\text{Au})=0.43(6)\ (\text{s K})^{-1}$ (Ref. 37), thus seems to be rather too small than too large, as previously assumed.

The relaxation constants of $^{189}$Os, $^{183}$W, and $^{181}$Ta, which were determined by SE-NMR, were also significantly larger than expected from the literature values of $R_m/g^2$. In the case of Os and Ta this may well be due to the quadrupolar contribution to the relaxation, which is larger for $^{189}$Os and $^{181}$Ta than for the isotopes that were used to derived $R_m/g^2$ ($^{193}$Os, $^{183}$Ta, and $^{182}$Ta). Only in the case of $^{183}$W the discrepancy must have another origin.

### ACKNOWLEDGMENTS

We wish to thank E. Smolic and P. Maier-Komor for experimental help. The support of the Forschungszentrum Jülich, Zentralabt. Forschungsreaktoren, is gratefully acknowledged.

[1] J. Korringa, Physica (Amsterdam) **16**, 601 (1950).
[2] Y. Obata, J. Phys. Soc. Jpn. **18**, 1020 (1963).
[3] Y. Yafet and V. Jaccarino, Phys. Rev. **133**, 1630 (1964).
[4] Y. Obata, J. Phys. Soc. Jpn. **19**, 2348 (1964).
[5] T. Asada and K. Terakura, J. Phys. F: Met. Phys. **12**, 1387 (1982).
[6] R. Markendorf, C. Schober, and W. John, J. Phys.: Condens. Matter **6**, 3965 (1994).
[7] I. Cabria, M. Deng, and H. Ebert, Phys. Rev. B **62**, 14 287 (2000).
[8] A. Narath and D. W. Alderman, Phys. Rev. **143**, 328 (1966).
[9] R. R. Hewitt and D. E. MacLaughlin, J. Magn. Reson. (1969-1992) **30**, 483 (1978).
[10] J. M. Keartland, G. C. K. Folscher, and M. J. R. Hoch, Phys. Rev. B **43**, 8362 (1991).
[11] V. R. Green and N. J. Stone, Hyperfine Interact. **30**, 355 (1986).
[12] R. Markendorf and C. Schober, J. Phys.: Condens. Matter **7**, 4561 (1995).
[13] G. Seewald, E. Zech, H.-J. Körner, D. Borgmann, M. Dietrich, and ISOLDE Collaboration, Phys. Rev. Lett. **88**, 057601 (2002).
[14] T. Funk, E. Beck, W. D. Brewer, C. Bobek, and E. Klein, J. Magn. Magn. Mater. **195**, 406 (1999).
[15] M. Kontani, T. Hioki, and Y. Masuda, J. Phys. Soc. Jpn. **32**, 416 (1972).
[16] H. D. Rüter, W. Haaks, E. W. Duczynski, E. Gerdau, D. Visser, and L. Niesen, Hyperfine Interact. **9**, 385 (1981).
[17] D. W. Murray, A. L. Allsop, and N. J. Stone, Hyperfine Interact. **11**, 127 (1981).
[18] F. Bacon, J. A. Barclay, W. D. Brewer, D. A. Shirley, and J. E. Templeton, Phys. Rev. B **5**, 2397 (1972).
[19] E. Matthias and R. J. Holliday, Phys. Rev. Lett. **17**, 897 (1966).
[20] E. Hagn and E. Zech, Phys. Lett. **101A**, 49 (1984).
[21] E. Klein, in *Low-Temperature Nuclear Orientation*, edited by N. J. Stone and H. Postma (North-Holland, Amsterdam, 1986), Chap. 12.
[22] K. S. Krane, in *Low-Temperature Nuclear Orientation*, edited by N. J. Stone and H. Postma (North-Holland, Amsterdam, 1986), Chap. 2.
[23] A. Bohr and V. W. Weisskopf, Phys. Rev. **77**, 94 (1950).
[24] G. J. Perlow, in *Hyperfine Interactions in Excited Nuclei*, edited by G. Goldring and R. Kalish (Gordon and Breach, New York, 1969), p. 651.
[25] H. Akai, M. Akai, S. Blügel, B. Drittler, H. Ebert, K. Terakura, R. Zeller, and P. H. Dederichs, Prog. Theor. Phys. Suppl. **101**, 11 (1990).
[26] A. Abragam and R. V. Pound, Phys. Rev. **92**, 943 (1953).
[27] G. Seewald, E. Zech, E. Hagn, and H.-J. Körner, Phys. Rev. B **68**, 014402 (2003).
[28] M. Kopp and E. Klein, Hyperfine Interact. **11**, 153 (1981).
[29] P. T. Callaghan, P. J. Back, and D. H. Chaplin, Phys. Rev. B **37**, 4900 (1988).
[30] P. J. Back, D. H. Chaplin, and P. T. Callaghan, Phys. Rev. B **37**, 4911 (1988).
[31] G. Seewald, E. Hagn, E. Zech, and D. Forkel-Wirth, Nucl. Phys. A **602**, 41 (1996).
[32] G. Seewald, E. Hagn, and E. Zech, Phys. Rev. B **63**, 054428 (2001).
[33] P. T. Callaghan, P. D. Johnston, W. M. Lattimer, and N. J. Stone, Phys. Rev. B **12**, 3526 (1975).
[34] P. Raghavan, At. Data Nucl. Data Tables **42**, 189 (1989).
[35] P. A. Vanden Bout, V. J. Ehlers, W. A. Nierenberg, and H. A. Shugart, Phys. Rev. **158**, 1078 (1967).
[36] H. Akai, Hyperfine Interact. **43**, 255 (1988).
[37] Y. Masuda, T. Hioki, and M. Kontani, Int. J. Magn. **6**, 143 (1974).